The stochastic entry of enveloped viruses: Fusion vs. endocytosis

Tom Chou

Depts. of Biomathematics & Mathematics, UCLA, Los Angeles, CA 90095

(Dated: February 8, 2008)

Viral infection requires the binding of receptors on the target cell membrane to glycoproteins, or "spikes," on the viral membrane. The initial entry is usually classified as fusogenic or endocytotic. However, binding of viral spikes to cell surface receptors not only initiates the viral adhesion and the wrapping process necessary for internalization, but can simultaneously initiate direct fusion with the cell membrane. Both fusion and internalization have been observed to be viable pathways for many viruses. We develop a stochastic model for viral entry that incorporates a competition between receptor mediated fusion and endocytosis. The relative probabilities of fusion and endocytosis of a virus particle initially nonspecifically adsorbed on the host cell membrane are computed as functions of receptor concentration, binding strength, and number of spikes. We find different parameter regimes where the entry pathway probabilities can be analytically expressed. Experimental tests of our mechanistic hypotheses are proposed and discussed.

I. INTRODUCTION

Viral entry mechanisms are typically classified as either endocytotic, or as fusogenic [1]. In the latter, the virus membrane, after association with the surface of the host cell, fuses and becomes contiguous with the cell membrane. This process is mediated by the binding of cell surface receptors to glycoprotein spikes on the viral membrane surface, forming fusion competent complexes spanning the viral and cell membranes. In endocytosis, the host cell first internalizes the virus particle, wrapping it in a vesicle before acidification-induced fusion with the endosomal membrane can occur. Wrapping can occur only after cell surface receptors, that also act as attachment factors, bind to the viral spikes. Experimentally, both fusion with the cell membrane and internalization can be observed and distinguished using microscopy [2, 3].

Many viruses, such as influenza and hepatitis B, use endocytosis as their primary mode of entry [4, 5]. The surface of an influenza virus is coated with ~ 400 hemagglutinin (HA) protein spikes [6]. The HA adheres to sialic acid-containing glycoproteins and lipids on the cell surface leading to wrapping of the virus particle. Particle wrapping may also be mediated by the recruitment of pit-forming clathrin/caveolin compounds [7]. Cell membrane pinch-off, leading to internalization of the virus, usually requires additional enzymes such as dynamin and endophilin [9]. Endosomal acidification oligomerizes the HA, priming them to fuse with the endosomal membrane. Direct fusion of the influenza virus with the host cell membrane is precluded since HA is activated only in the acidic endosomal environment. However, low pH conditions have also been shown to induce the direct fusion of influenza virus with certain cells [10].

Recent experiments on the avian leukosis retrovirus (ALV) have provided evidence both for a pH-dependent direct fusion mechanism [11, 12], and an endocytotic pathway [13]. Moreover, the entry pathway of some viruses such as Semliki Forest Virus (SFV) can be shifted from endocytosis to fusion by acid treatment, but only in certain host cell types [14]. In this case, low pH triggering of receptor-primed envelope glycoproteins can initiate fusion before the virus

can be wrapped and endocytosed. Vaccinia and HIV (typically infecting cells via direct fusion) have also been shown to exploit both entry mechanisms [7, 15, 16, 17]. For example, fusion-independent mechanisms of HIV-1 capture and internalization in mature dendritic cells, mediated by DC-SIGN [18], can be a significant mode of HIV transmission through dendritic cells and lymphatic tissue [19]. Capture by DC-SIGN and CLEC-2 adhesion molecules also internalizes HIV in platelets [20]. Thus, depending upon physical conditions and cell type, both entry pathways are potentially accessible to certain viruses. The choice seems to depend on the type of receptors the viruses engages, whether they are receptors/coreceptors that induce fusion (perhaps triggered by low pH), or simply attachment factors such as sialic acid-rich glycoproteins that do not induce fusion. In this latter case, complete wrapping before an irreversible fusion event is more likely to occur, and internalization is favored.

It is not surprising that subtle changes in the interactions between viral membrane proteins and cell receptors dramatically affect the infectivity of a virus, as recently demonstrated for the 1918 influenza virus [21]. In this paper, we model virus-receptor kinetics and propose a mechanism consistent with the above experimental observations, and that describes viral entry by incorporating both fusion and endocytosis entry pathways in a probabilistic manner. In the next section, we develop a stochastic one-species receptor model for the binding of receptors necessary to start the virus wrapping process. These receptors, upon binding, can induce membrane fusion at each receptor-spike complex. In the Results, we find parameter regimes in which each of the entry mechanisms dominate. Explicit expressions for the entry pathway probabilities, as functions of the relevant kinetic rates, are given in the Appendix. In the Discussion and Summary, we explore the connection between our parameters and experimentally controllable physical conditions such as receptor/coreceptor density, spike density, and cell membrane rigidity. Experimental tests are proposed and extensions of our analysis to more realistically incorporate biological features are discussed.
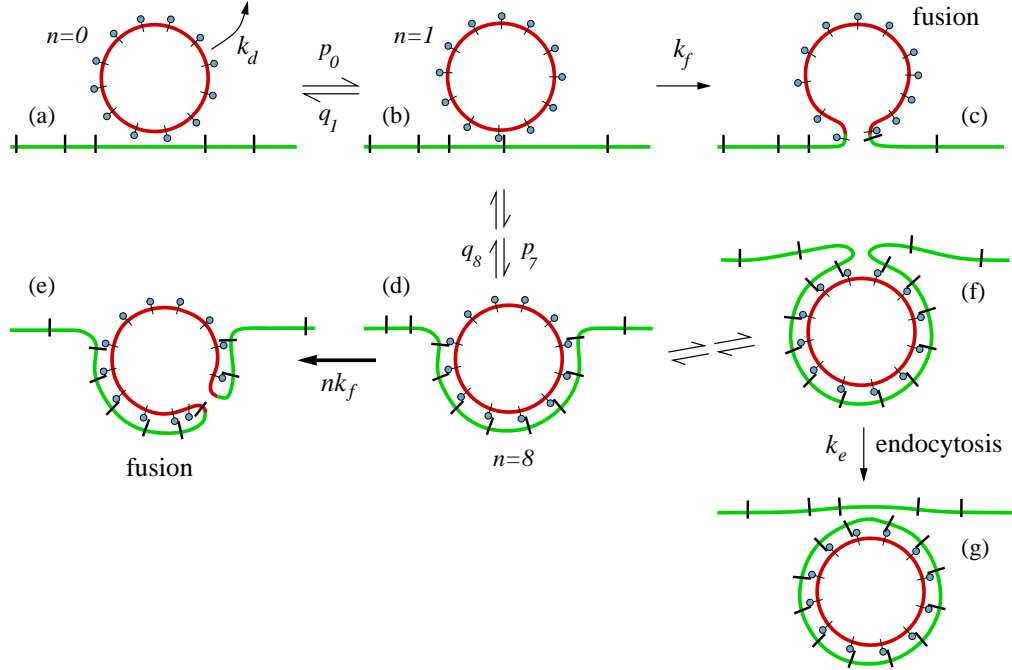
FIG. 1: A schematic of viral entry pathways. (a) A nonspecifically adsorbed virus particle can desorb with rate k_d, or it can (b) recruit and specifically bind a receptor. The receptor can immediately initiate membrane fusion with rate k_f as shown in (c), or, it can recruit additional receptor molecules, inducing wrapping of the virus particle. From partially wrapped states (d), the virus can at any stage undergo membrane fusion (e), or, it can completely wrap and internalize the virus particle ((f) and (g)).

II. SINGLE RECEPTOR KINETIC MODEL

The basic features of our proposed mechanism are shown in Fig. 1. A virus particle initially nonspecifically adsorbed on the cell membrane (without any bound receptors) can spontaneously dissociate with rate k_d. Alternatively, mobile receptors in the cell membrane can bind specifically to the glycoprotein spikes (assumed here to be uniformly distributed) on the viral surface. Successive addition of receptors to the viral ligands, when n are already attached, occurs with rate p_n. Thus, the binding of the first receptor occurs with rate p_0. Similarly, desorption of the nth receptor occurs at rate q_n. We consider the adsorption of a single effective receptor or attachment factor to a spike, lumping together the effects of multiple receptor/coreceptor types. This approximation is valid when, for example, coreceptor binding is highly cooperative such as suggested in the HIV infection process where CD4 binding to the gp120 protein spike induces rapid CCR5 coreceptor binding [22].

Receptors not only adhere the cell membrane to the viral membrane, but can also initiate local membrane fusion at each receptor-spike complex with rate k_f. Fusion can occur at any time during the receptor recruitment process and is more likely to occur per unit time with more bound receptors. Receptor-spike complexes that are unable to initiate fusion are described by a vanishing fusion rate $k_f \to 0$. However, if receptors have high fusogenicity k_f, the virus might fuse only after a single receptor has attached. Only if the system reaches a fully wrapped state with N bound

receptors (Fig. 1f), before any fusion event occurs, can pinch-off and endocytosis occur with rate k_e. The number of spikes N is typically large, varying among viruses such as HIV ($N \sim 15$)[23], SIV ($N \sim 70$)[23], and Influenza ($N \sim 400$)[6]. The path to endocytosis is thus a race between fusion and complete wrapping of a relatively large number N of viral spikes.
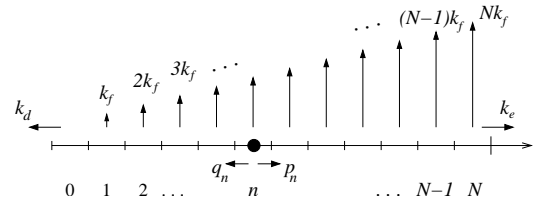

FIG. 2: The stochastic process representing the competition between membrane fusion and endocytosis. The states n correspond to the number of receptor-spike complexes formed, while N is the total number of spikes on the virus membrane. Each receptor-spike complex can initiate membrane fusion with rate k_f. As more receptors are bound, the total rate of fusion increases linearly. The irreversible pinch-off and endocytosis rate is denoted k_e.

States in the model are labeled by the index n (Fig. 2), representing the number of formed receptor-spike complexes. Starting from a nonspecifically adsorbed virus particle denoted by state $n = 0$, the system progresses along the chain with the appropriate transition rates corresponding to attachment and detachment of cell membrane receptors.

The probability $P_n(t)$ of having n bound receptors (or attachment factors) at time t obeys the master equation

$$\dot{P}_n(t) = -(nk_f + p_n + q_n)P_n + p_{n-1}P_{n-1}$$

$$+q_{n+1}P_{n+1}, \quad 1 \leq n \leq N-1,$$

$$\dot{P}_0(t) = -(k_d + p_0)P_0 + q_1 P_1,$$

$$\dot{P}_N(t) = -(Nk_f + k_e + q_N)P_N + p_{N-1}P_{N-1}.$$

(1)

Although we describe the general viral entry process in terms of recruitment and binding of a single type of receptor, our model encompasses processes involving clathrin or calveolin aggregation and pit formation, typically leading to endocytosis. All of these biologically distinct, but physically similar mechanisms can be analyzed by appropriately interpreting the rates. For example, the nucleation of a clathrin-coated pit can be modeled by effective binding and unbinding rates p_n and q_n that describe the rates of clathrin addition and removal from the pit. Since individual clathrin molecules are not known to induce membrane fusion, the fusion rate $k_f = 0$, and only endocytosis (or virus dissociation from the cell surface) would occur. The fusion rate is also negligible if the receptor is a simple attachment factor that adheres the membranes, but does not facilitate fusion.

The receptor binding and unbinding rates, p_n and q_n, are related to the cell surface receptor density and the receptor-spike binding strength, respectively. The Markov process shown in Fig. 2 implicitly assumes that the receptor recruitment is not diffusion-limited – the rate of addition of successive receptors is independent of the history of previous receptor bindings.

Approximate forms for p_n, q_n can be physically motivated by considering the number of ways additional receptors can bind or unbind, given that there already exist n receptor-spike complexes. As the membrane progressively wraps around the virus particle, the rate of addition of the next receptor is proportional to the number n_p of unattached spikes bordering the virus-cell membrane contact line L, as shown in Fig. 3.

For a large number N of uniformly distributed spikes on a virus particle of radius R, the contact area $A_c \approx 4\pi R^2 n/N \approx 2\pi R^2(1 - \cos\theta_n)$ where $\theta_n = \cos^{-1}[1 - 2n/N]$ is the angle subtended by the contact line when n receptors are attached. Since the area per spike is $a_s \approx 4\pi R^2/N$, the number of spikes near the contact perimeter $L = 2\pi R \sin\theta_n$ is found from $n_p \approx L/\sqrt{a_s}$. Upon using the explicit form for θ_n, we find the number n_p of periphery spikes as a function of $n \geq 1$ receptor-bound spikes, $n_p \sim \sqrt{\pi N}\sqrt{1 - (1 - 2n/N)^2}$. At a stage where $n \geq 1$ receptors have bound, approximately n_p spikes are accessible for additional binding of receptors. Similarly, there are approximately n_p receptor-spike complexes available for dissociation. Combinatorially, the receptor binding and unbinding rates take the form [24]
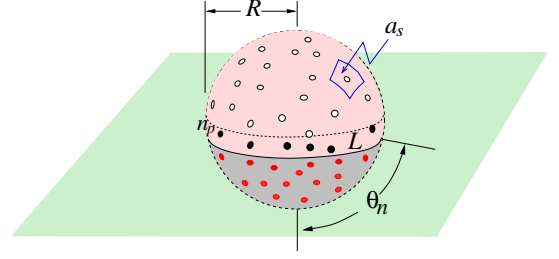

FIG. 3: Schematic of a partially wrapped virus particle. The unbound spikes above the contact region are represented by open circles, while the receptor-bound spikes in the contact region are represented by the red-filled circles. The number n_p of spikes or spike-receptor complexes near the contact perimeter used to compute p_n or q_n via Eqs. 2 are shown as black dots.

$$p_n \approx p_0 \frac{\sqrt{1 - \left(1 - \frac{2n}{N}\right)^2}}{\sqrt{1 - \left(1 - \frac{2}{N}\right)^2}}, \quad q_n \approx q_1 \frac{\sqrt{1 - \left(1 - \frac{2n}{N}\right)^2}}{\sqrt{1 - \left(1 - \frac{2}{N}\right)^2}}, \quad (2)$$

where $1 \leq n \leq N-1$, p_0 is the intrinsic rate of binding the first receptor, and $q_1 = q_N$ is the dissociation rate of an individual receptor-spike complex. Since q_1 is a spontaneous receptor-spike dissociation rate, it is independent of receptor density and spike number. If the receptor-spike binding energy is at least a few k_BT, we also expect q_n to be relatively insensitive to the cell membrane bending rigidity.

A number of physical attributes and biological intermediates can be incorporated into the rate parameters to address more complicated microscopic processes. For example, if thermal fluctuations are rate-limiting, there would be an additional factor in p_n reflecting the probability per unit time that a patch of membrane fluctuates to within a distance of the virus surface spike that allows receptor-spike binding. The dynamics of this process depends on the cell membrane tension and rigidity, the typical spike spacing, and potentially the viscosity of the extracellular environment. For stiff membranes under tension, the wrapping of spherical particles encounters an energy barrier near half-wrapping [25], which can be incorporated into the dynamics by assuming an additional factor in p_n that has a minimum near $n \approx N/2$. Thus, the energy barrier associated with membrane bending will tend to flatten the n-dependence of p_n.

Particular aspects of the entry process can also influence estimates of the other rates. If the viral spikes are mobile and can aggregate to the initial focal point of adhesion, the target cell membrane is not able to fully wrap and endocytosis is prevented. The overall kinetic scheme remains unchanged except with $k_e \approx 0$. Finally, the recruitment of secondary coreceptors that occurs in, e.g. HIV fusion, can also be developed within our current framework and is discussed in the Discussion and Summary section. Although some of the physical details described above influence the specific values of p_n, we will show that for large N, the qualitative behavior of our model can be summarized by distinct pa-
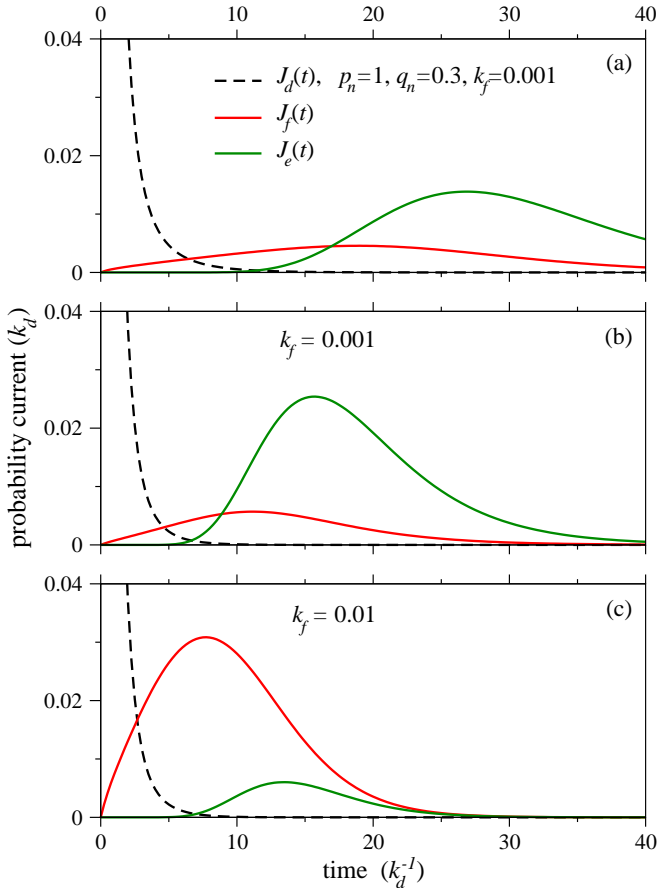
FIG. 4: The currents through each pathway for $N = 20$ spikes. The dashed black curve is the current for desorption, while the red and green curves are the currents for fusion and endocytosis, respectively. Time is measured in units of k_d^{-1}, and all rates are normalized with respect to k_d. The parameters used in all plots are $p_0 = 1$, $q_1 = 0.3$, and $k_e = 0.3$. (a) The currents for constant $p_n = 1$, $q_n = 0.3$ and fusion rate $k_f = 0.001$. (b) The same parameters except that Eqs. 2 are used for the rates p_n, q_n. (c) The currents with p_n, q_n as in (b), except that the fusion rate of each spike-receptor complex is increased to $k_f = 0.01$.

rameter regimes, somewhat insensitive to the precise values of p_n, q_n.

III. RESULTS

We solved Eq. 1 for the probabilities $P_n(t)$ given an initial condition $P_n(t = 0) = \delta_{n,0}$. Using these probabilities, we find the probability currents through the dissociation, fusion, and endocytosis pathways, $J_d(t) = k_d P_0(t)$, $J_f(t) = k_f \sum_{n=1}^{N} n P_n(t)$, and $J_e(t) = k_e P_N(t)$, respectively. Figure 4 shows the current for each pathway as a function of time (in units of k_d^{-1}). Note that detachment, fusion, and endocytosis arise sequentially in time. Upon comparing Fig 4(a) and (b), we see that changing p_n, q_n from constant values to the forms in Eqs. 2 shifts the currents through the fusion and endocytotic pathways to earlier times. This
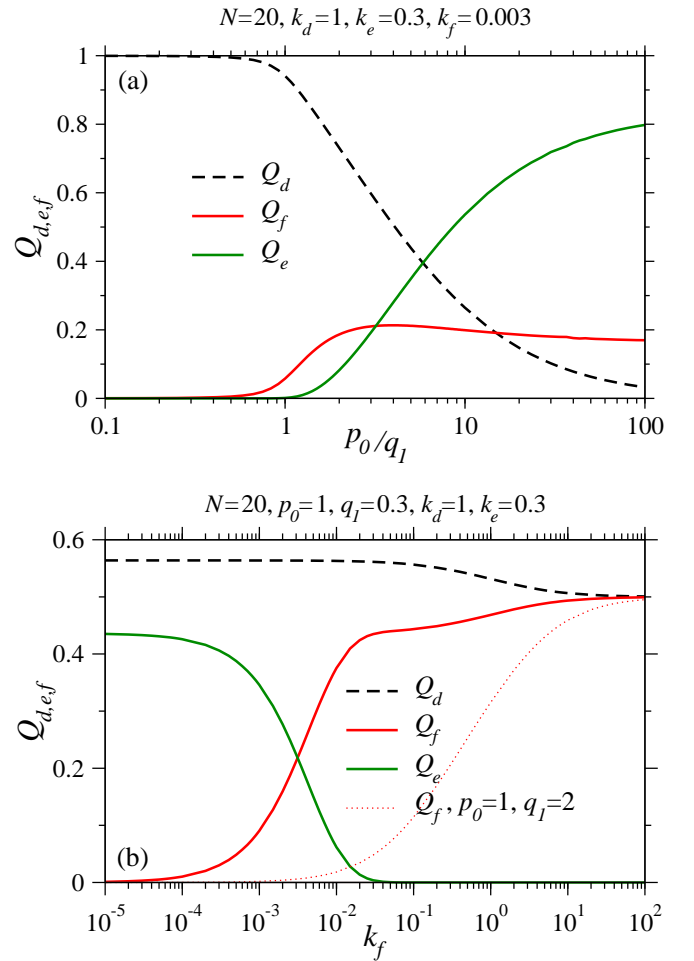
FIG. 5: Numerical solutions of entry probabilities Q_i (all rates normalized by k_d). (a) The entry probabilities as a function of p_0. Endocytosis arises only for larger $p_0 > q_1$, after the fusion probability becomes significant. Parameters used are $N = 20, k_f = 0.003, k_e = 0.3$ (all rates are normalized by k_d). (b) The probabilities of dissociation (dashed), fusion (red), and endocytosis (green) as functions of the individual receptor-spike fusion rate k_f. Here, $q_1 = 0.3$. The thin dashed red curve corresponds to a faster receptor detachment rate ($q_1 = 2$) which prevents endocytosis.

speed-up is simply a consequence of the larger hopping rates p_n, q_n, especially for $n \approx N/2$. Nonetheless, the specific form of p_n, q_n, provided they are slowly varying in n, only quantitatively affect the timing of the onset of the currents. The dramatic variations in the infection pathway taken come with changes in k_f. When the fusion rate k_f is increased, endocytosis is suppressed in favor of fusion as shown by Figs. 4(b) and 4(c).

Upon time-integrating the currents, we find the total probabilities $Q_i = \int_0^\infty J_i(t)dt, (i = d, e, f)$ for each pathway. Note that from probability conservation, $Q_d + Q_e + Q_f = 1$. In Figure 5, we use the binding and unbinding rates given by Eqs. 2 to numerically compute the entry pathway probabilities Q_i. Fig. 5(a) shows the pathway probabilities as a

function of the intrinsic receptor binding rate p_0/q_1. This ratio is a measure of the density-dependent free energy ΔG of the spike-receptor binding: $p_0/q_1 \sim e^{\Delta G/kT}$ [24]. In the simplest limit of extremely low receptor density, ($p_0 \to 0$), $Q_d \sim 1 - \mathcal{O}(p_0), Q_f \sim \mathcal{O}(k_f p_0)$, and $Q_e \sim 0$, and only dissociation can occur. As p_0 is increased, the probability of fusion increases at the expense of desorption. Endocytosis remains negligible as long the states that occur with any appreciable probability are those with small n. Only as $p_0 \gg q_1$ does the probability of endocytosis become appreciable and approach the asymptotic expression given by Eq. 3 in the Appendix.

Figure 5(b) shows the total probabilities Q_d of dissociation, Q_f of fusion, and Q_e of endocytosis as functions of the fusion rate k_f. For large detachment rates (e.g. $q_1 = 2 > p_0 = 1$), $Q_e \approx 0$, and fusion can occur only at large k_f, as shown by the thin dotted curve. For the parameters used, $N = 20, p_0 = 1, q_1 = k_e = 0.3$ (normalized by k_d), the transition from a predominantly endocytotic pathway to a predominantly fusion pathway occurs for $10^{-3} \lesssim k_f \lesssim 10^{-2}$. When $k_f \gg 10^{-2}$, the sum of fusion probabilities over all intermediate states is appreciable, preventing endocytosis. Therefore, only for a particularly small fusion rate k_f, and nonnegligible endocytosis rate k_e is internalization possible. We show in the Appendix that generally, if $p_n > q_n$, the effective drift of the stochastic system towards the wrapped state renders the partitioning between fusion and endocytosis controlled by the fusion rate k_f. If this is the case, the transition from endocytosis to fusion occurs at approximately $k_f \sim (p_n + q_n)/N^2$, as is confirmed by the numerical solution for $N = 20$ shown in Fig. 5(b).

Although we have chosen $N = 20$ as a representative spike number, different viruses and their variants can have a widely varying number of active spikes. In Fig. 6 we show how the entry pathway probabilities depend on the number N of active viral spikes. As N is increased, the probability for fusion increases at the expense of endocytosis. For $N \to \infty$, and a nonzero k_f, $Q_e \to 0$ since fusion will likely occur during the infinitely long wrapping processes. For small N, the plotted probabilities must be interpreted with an N-dependent k_e. Suppose $N \lesssim 10$. Even if all spikes are receptor-bound, the membrane has an appreciable distance to bend and before full wrapping and endocytosis can occur. Effectively, the fusion rate k_e starts to decrease if N gets small such that the rate of membrane fluctuations over a typical interspike distance decreases.

Provided $p_n - q_n \gg 1/N$, asymptotic analysis of the solutions reveal qualitatively different behaviors depending upon how the fusion rate k_f compares with $1/N$. If the receptor-spike complex is highly fusion competent such that $k_f/(p_n + q_n) \gg 1/N$, the probability of reaching a completely wrapped ($n \approx N$) state is exponentially small and endocytosis cannot occur. Here, the virus pathway is nearly entirely partitioned between dissociation and fusion, as indicated by the asymptotic expressions for Q_i given by Eqs. 4 in the Appendix.

If $1/N^2 \ll k_f/(p_n + q_n) \ll 1/N$, the receptor-spike complex has intermediate fusogenicity. In this case, the time-integrated probability $\int_0^\infty P_n(t)\mathrm{d}t$ used to construct Q_i re-
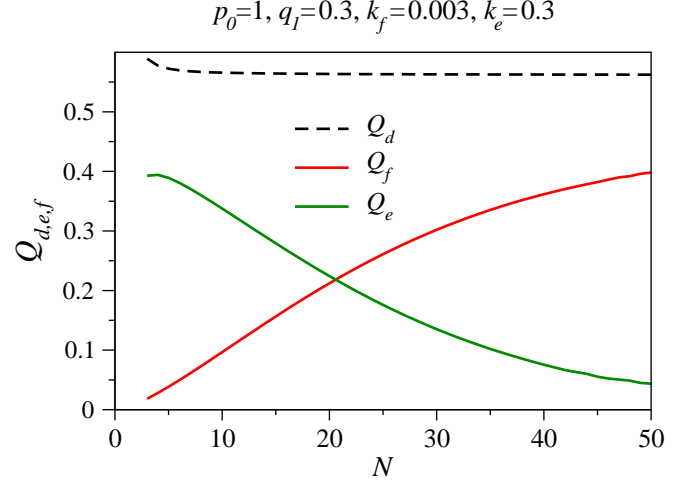

$p_0{=}1, q_I{=}0.3, k_f{=}0.003, k_e{=}0.3$

FIG. 6: The pathway dependence on receptor association/dissociation rates and the number N of virus spikes. The number of spikes controls which regime Eq. 4 or Eq. 5 is valid. Large N enhances fusion almost entirely at the expense of endocytosis.

mains small for $n \approx N$ and the probability of endocytosis is still exponentially small, despite the smaller k_f. In this regime, we find in the Appendix (Eq. 5), an expression for Q_d. Only when $k_f/(p_n + q_n) \ll 1/N^2$ is virus internalization appreciable. Expressions for Q_f and Q_e in this very weak fusogenicity limit are also displayed in Eq. 5 of the Appendix. The expression we find agree with the exact numerical evaluation of $Q_{d,e,f}$ from solving Eq. 1.

IV. DISCUSSION AND SUMMARY

Fusion can be directly distinguished from endocytosis by imaging fluorescent markers loaded into viruses or model vesicles. Upon fusion, one expects to see an immediate release of marker into the periphery of the target cell. Similarly, single-liposome fluorescence imaging experiments that label and detect vesicle lipids and as they mix with a supported bilayer upon fusion [26], can be used as *in vitro* model systems for virus fusion. In such experiments, the model parameters p_n, q_n, k_f, k_e, k_d can be tuned by controlling certain physical chemical properties, enabling one to dissect the mechanism of viral entry. The entry pathways delineated by the different parameter regimes described in the previous section, and by the asymptotic formulae given in the Appendix, provide a framework for analyzing and designing viral entry experiments.

The receptor density plays the first critical role via the binding rate parameter p_n. For low receptor densities, and proportionately lower p_n (but fixed spontaneous detachment rate q_n), the virus particle can only dissociate or fuse. Although lowering receptor concentration decreases the overall entry probability, it can increase Q_f/Q_e, the fusion probability relative to endocytosis probability (see Fig. 5(a)). Only for $p_n - q_n > O(1/N)$ can the receptor spike complex fusion

rate k_f become important in determining whether fusion or endocytosis occurs. In order for endocytosis to occur, the fusion rates must be small such that $k_f/(p_n + q_n) \ll 1/N^2$. The rate p_n can also be substantially decreased by increasing the target membrane surface tension, thereby suppressing the thermal fluctuations of the membrane required to bring cell receptors and viral spikes into proximity.

The rapid drop-off in endocytosis predicted as the fusion rate is increased from $k_f/(p_n + q_n) \ll 1/N^2$ to $k_f/(p_n + q_n) \gg 1/N^2$, especially for large N, shows that tuning physical conditions (such as pH or temperature) that affect the fusogenicity of receptor-spike complexes, k_f, can have a large effect on the viral entry pathway. Recent experiments by Melikyan *et al.* [27], Henderson and Hope [28], and others have shown a rate-limiting intermediate in the HIV fusion process that can be arrested by lowering temperature. Since CD4 binding was not the rate limiting step, lowering the temperature decreases k_f to a degree presumably much less that $(p_n + q_n)/N^2$, preventing fusion. If these systems have the necessary endocytotic machinery and support pinch-off, lowering temperature and arresting the receptor-spike fusion complex while retaining the adhesive wrapping of receptor-spike binding would enhance the endocytotic pathway. The effective rate k_f can also be lowered by cross-linking (with *e.g.*, defensins) membrane glycoproteins, rendering their complexes with viral spikes fusion incompetent [29]. However, if the cross-linked glycoproteins retain their attraction for the viral surface, the probability of wrapping and internalization would increase. If an independent measurement or estimate of $p_n + q_n$ is available, the dependence of k_f on temperature, pH, and chemical modification can be probed.

Finally, pathways to fusion and endocytosis can diverge for systems that require both primary receptors and secondary receptors (coreceptors). If two species are required, one for adhering cell and viral membranes, and another to induce fusion, endocytosis will be favored, all else being equal. In this case, the initial receptor binding only causes the cell membrane to wrap around the virus particle. An additional coreceptor must diffuse and bind to the spike-receptor adhesion complex to induce fusion. A highly cooperative receptor-coreceptor interaction, such as in HIV fusion involving CD4 and CCR5/CXCR4, is still modeled by Eq. 1, but with the binding rates p_n interpreted as an effective binding rate for both classes of receptor, proportional to the product of their surface concentrations. However, if the coreceptor density and/or mobility is limiting [17], the binding of receptors occur first, with coreceptor priming and formation of a fusion competent receptor-spike complex occurring slowly. This allows time for receptor (adhesion molecule) mediated membrane wrapping of the entire virus, enhancing the likelihood of endocytosis. Thus, by maintaining a high adhesion receptor density, and lowering the fusion-enabling coreceptor density, one enhances the endocytotic pathway.

V. APPENDIX

Consider the Master Equation 1 in the form $\dot{\mathbf{P}}(t) = -[\mathbf{M}_0 + \mathbf{M}_f]\mathbf{P}$, where $\mathbf{M}_0$ is the conserved random walk transition matrix involving only k_d, p_n, q_n, and k_e, and $\mathbf{M}_f = k_f \text{diag}(n)$ is decay term arising from fusion. Large N expressions for the entry pathway probabilities Q_i can be obtained in different limits.

In the limit where the receptor binding is irreversible ($p_n/q_n \to \infty$), Eq. 1 can be solved exactly:

$$Q_d = \frac{k_d}{p_0 + k_d}$$

$$Q_f = \frac{1}{p_0 + k_d}\left[p_0 - \frac{k_e p_{N-1}}{k_e + Nk_f}\prod_{m=1}^{N-1}\frac{p_{m-1}}{p_m + mk_f}\right] \qquad (3)$$

$$Q_e = \frac{k_e}{k_e + Nk_f}\frac{p_{N-1}}{p_0 + k_d}\prod_{m=1}^{N-1}\frac{p_{m-1}}{p_m + mk_f}.$$

If $q_n = 0$, the probability of dissociation is fixed by k_d and p_0, and the remaining current is partitioned between fusion and endocytosis. For a given p_0, k_f, k_e, this limit gives the highest probability of the maximally-wrapped state and the highest endocytosis probability.

When $p_n - q_n \gg 1/N$, there are two possible limits corresponding to high receptor-spike fusion rates, $k_f/(p_n + q_n) \gg 1/N$, and intermediate fusion rates $1/N \gg k_f/(p_n + q_n) \gg 1/N^2$. For $k_f/(p_n + q_n) \gg 1/N$, $\int_0^\infty P_n(t)dt$ is nonnegligible only for $n \approx 0$ and $\int_0^\infty P_N(t)dt$ is exponentially small. A small n local analysis of Eq. 1 yields

$$Q_d \approx \frac{k_d}{k_d + p_0 - p_0 q_1/(p_1 + q_1)}$$

$$Q_f \approx \frac{p_0}{k_d + p_0 + k_d q_1/p_1}, \qquad \text{and} \qquad (4)$$

$$Q_e \approx 0, \qquad\qquad \text{for} \quad \frac{k_f}{p_n + q_n} \gg 1/N,$$

explicitly showing the absence of endocytosis. The values for Q_d and Q_f corresponding to the parameter values used in Fig. 6 are $Q_d \approx 0.56$ and $Q_f \approx 0.435$, which agree well with the large N limit of the numerical soution.

In an intermediate fusogenicity regime, $1/N \gg k_f/(p_n + q_n) \gg 1/N^2$, $\int_0^\infty P_n(t)dt$ is nearly constant for $n \ll N$. However, $\int_0^\infty P_N(t)dt$ remains small and endocytosis, although still unlikely, occurs with slightly higher probability than in the high fusogenicity limit. In this intermediate limit, one might first attempt perturbation theory about $k_f = 0$ (since its largest element of $\mathbf{M}_f$, $Nk_f \ll p_n + q_n$, is much small than the typical elements of $\mathbf{M}_0$). However, as $1/N$ decreases, so do the spacings between eigenvalues of the zero-fusion transition matrix $\mathbf{M}_0$. Heuristically, for perturbation theory to be accurate for slowly varying p_N, q_N, the largest of the diagonal correction terms, Nk_f, must be smaller than $(p_n + q_n)/N$, the typical spacing between eigenvalues. First order perturbation for *all* $P_n(t)$ is accurate

only if $k_f/(p_n + q_n) \ll 1/N^2$, as is explicitly shown by Eqs. 3. Upon expanding Q_f and Q_e (from Eqs. 3) in powers of k_f, one finds $\mathcal{O}(N^2)$ corrections terms. Thus, the expansion is only accurate if $k_f/(p_n + q_n) \ll 1/N^2$. Endocytosis is preempted by fusion or dissociation only when perturbation theory about a nonnegligible Q_e fails (when $k_f/(p_n + q_n) \not\ll 1/N^2$). Perturbation results for the few-

receptor states $n \approx 0$ important for the dissociation probability Q_d, are still valid as long as $k_f/(p_n+q_n) \ll 1/N$. However, the perturbation results that include the flux through larger ($n \approx N$) states are accurate only if the receptor-spike complexes are extremely inefficient at initiating membrane fusion, and $k_f/(p_n + q_n) \ll 1/N^2$. Thus, for small enough $k_f/(p_n + q_n)$, we find

$$Q_d \approx \frac{k_d + k_d \sum_{n=1}^{N-1} \prod_{i=1}^{n}(q_i/p_i) + (k_d q_N/k_e)\prod_{i=1}^{N-1}(q_i/p_i)}{k_d + p_0 + k_d \sum_{n=1}^{N-1}\prod_{i=1}^{n}(q_i/p_i) + (k_d q_N/k_e)\prod_{i=1}^{N-1}(q_i/p_i)}, \quad k_f/(p_n+q_n) \ll N^{-1}$$

$$Q_f \approx \frac{p_0 - q_1}{k_d + p_0 - q_1} - Q_e, \qquad\qquad k_f/(p_n+q_n) \ll N^{-2} \quad \text{where} \tag{5}$$

$$Q_e \approx \frac{k_e}{k_e + p_0^{-1}k_d k_e \left[1 + \sum_{j=1}^{N-1}\prod_{i=1}^{j}\left(\frac{q_i}{p_i}\right)\right] + k_d \prod_{j=0}^{N-1}\left(\frac{q_{j+1}}{p_j}\right)}, \quad k_f/(p_n+q_n) \ll N^{-2},$$

independent of k_f. Equations 3-5 give estimates for the entry probabilities $Q_{d,e,f}$ in the different parameter regimes. For small N such that $k_f/(p_n + q_n) \ll N^{-2}$, $Q_e \approx 0.411$, which agrees well with the limit shown in Fig. 6.

[1] Barocchi MA, Masignani V, Rappuoli R (2005) *Nature Reviews Microbiology* 3:349-358.
[2] Lakadamyali M, Rust MJ, Babcock HP, Zhuang X (2003) *PNAS* 100:9280-9285.
[3] Markosyan RM, Cohen FS, Melikyan GB (2005) *Mol. Biol. Cell.* 16:5502-5513.
[4] Cross KJ, Burleigh LM, Steinhauer DA (2001) *Expert Reviews in Molecular Medicine* August 6, 1-18.
[5] Shekel JJ, Wiley DC (2000) *Ann. Rev. Biochem.* 69:531-569.
[6] Masaki I, Mizuno T, Kawasaki K (2006) *J. Biol. Chem.* 281:12729-12735.
[7] Dimitrov DS (2004) *Nature Reviews* 2:109-122.
[8] Sens P, Turner MS (2004) *Biophys. J.* 86:2049-2057.
[9] Praefcke GJK, McMahon HT (2004) *Nature Reviews in Molecular Cell Biology* 5:133-147.
[10] Duzgunes N, Pedroso de Lima MC, Stamatatos L, Flasher D, Alford D, Friend DS, Nir S (1992) *J. Gen. Virology* 73:27-37.
[11] Melikyan GB, Barnard RJO, Markosyan RM, Young JAT, Cohen FS (2004) *J. Virol.* 78:3753-3762.
[12] Mothes W, Boerger AL, Narayan S, Cunningham JM, Young JAT (2000) *Cell* 103:679-689.
[13] Diaz-Griffero F, Hoschander SA, Brojatsch J (2002) *J. Virol.* 76:12866-12876.
[14] Marsh M, Bron R (1997) *J. Cell Sci.* 110:95-103.
[15] Lai C, Gong S, Esteban M (1991) *J. Virology* 65:499-504.
[16] Schaeffer E, Soros VB, Greene WC (2004) *J. Virology* 78:1375-1383.
[17] Platt EJ, Durnin JP, Kabat D (2005) *J. Virology* 79:4347-4356.
[18] Su SV, Hong P, Baik S, Negrete OA, Gurney KB, Lee B (2004) *J. Biol. Chem.* 279:19122-19132.
[19] Geijtenbeek TB, Kwon DS, Torensma R, van Vliet SJ, van Duijnhoven GC, Middel J, Cornelissen IL, Nottet HS, Kewal-Ramani VN, Littman DR, Figdor CG, van Kooyk Y (2000) *Cell* 100:587-597.
[20] Chaipan C, Soilleux EJ, Simpson P, Hofmann H, Gramberg T, Marzi A, Geier M, Stewart EA, Eisemann J, Steinkasserer A, Suzuki-Inoue K, Fuller GL, Pearce AC, Watson SP, Hoxie JA, Baribaud F, Pohlmann S (2006) *J. Virology* 80:8951-8960.
[21] Tumpey TM, *et al.* (2007) *Science* 315:655 - 659.
[22] Kuhmann SE, Platt EJ, Kozak SL, Kabat D (2000) *J. Virology* 74:7005-7015.
[23] Zhu P, Liu J, Bess J, Chertova E, Lifson JD, Grisé H, Ofek GA, Taylor KA, Roux KH (2006) *Nature* 441:847-852.
[24] D'Orsogna MR, Chou T (2005) *Phys. Rev. Lett.* 95:170603.
[25] Deserno M (2004) *Phys. Rev. E* 69:031903.
[26] Yoon TY, Okumus B, Zhang F, Shin YK, Ha T (2006) *PNAS* 103:19731-19736.
[27] Melikyan GB, Markosyan RM, Hemmati H, Delmedico MK, Lambert DM, Cohen FS (2000) *J. Cell Biol.* 151:413-423.
[28] Henderson HI, Hope TJ (2006) *Virology J.* 3:36.
[29] Leikina E, Delanoe-Ayari H, Melikov K, Cho MS, Chen A, Waring AJ, Wang W, Xie Y, Loo JA, Lehrer RI, Chernomordik LV (2005) *Nature Immunology* 6:995-1001.